SCIENTIFIC Publishing Limited

Trends in Immunotherapy

https://ojs.ukscip.com/index.php/ti

Article

Histopathological Evaluation of the Neuroprotective Effects of Moringa Leaf Extracts in Methotrexate-Induced Hippocampal Damage in Albino Rats

Khlood M Mehdar

Department of Anatomy, Faculty of Medicine, Najran University, Najran 61441, Kingdom of Saudi Arabia

* Correspondence: Khlood.Mehdar02@gmail.com, Kmmehdar@nu.edu.sa

Received: 14 July 2025; **Revised:** 21 July 2025; **Accepted:** 30 July 2025; **Published:** 4 September 2025

Abstract: Methotrexate is a widely utilized chemotherapeutic agent known to induce neurotoxic effects, thereby constraining its therapeutic potential across various malignancies. While Moringa leaf extract has demonstrated significant antioxidants and anti-inflammatory properties, its role in mitigating Methotrexate-induced neurotoxicity remains inadequately explored. This study seeks to elucidate the protective effects of Moringa leaf extract on Methotrexate-mediated damage within the dentate gyrus of the hippocampus. Male rats were administered Moringa leaf extract at 300 mg/kg body weight via oral gavage bi-weekly over four weeks. Concurrently, select groups received intraperitoneal injections of 0.5 mg/kg Methotrexate twice weekly for the study. The administration of Methotrexate elicited oxidative stress, as evidenced by elevated levels of malondialdehyde and diminished activity of superoxide dismutase. Histopathological assessments revealed that Methotrexate treatment induced significant alterations in the dentate gyrus, characterized by an inflammatory response marked by the upregulation of Toll-like receptor 4. Activation of the Toll-like receptor 4 signalling pathway consequently led to an increased expression of the Nucleotide-binding oligomerization domain-like receptor family pyrin domain-containing 3-inflammasome and enhanced caspase-1 activation. Importantly, co-administration of Moringa leaf extract with Methotrexate substantially reduced both inflammatory and oxidative stress markers while restoring the dentate gyrus's structural integrity. Moringa leaf extract demonstrates potent antioxidant and anti-inflammatory properties that effectively counteract Methotrexate-induced neurotoxicity by modulating the brain's TLR4/NLRP3/caspase-1 signalling axis.

Keywords: Moringa Leaf Extract; Dentate Gyrus; Methotrexate Antioxidant; Anti-Inflammatory

1. Introduction

Methotrexate (MTX) is a well-characterized chemotherapeutic agent with anti-metabolite, anti-folate, and anti-tumor properties [1]. Its main mechanism is to inhibit cancer cell proliferation, and it also has neurotoxic effects. MTX is widely used in the treatment of different malignancies (e.g., acute lymphoblastic leukaemia) and the management of autoimmune and inflammatory disorders (e.g., psoriasis, rheumatoid arthritis) [2,3]. In addition, MTX interferes with the metabolism of neoplastic cells and modulates immune responses [4].

MTX is explicitly an inhibitor of dihydrofolate reductase, which, when entering cells, disrupts folic acid biosynthesis, an essential nucleotide precursor for DNA and RNA synthesis. This causes a disruption in cell proliferation [5]. In particular, the incidence of neurotoxicity has risen in parallel with the use of more aggressive treatment regimens [6]. According to Hwang et al. [7], MTX treatment leads to neurological and cognitive deficits that cause

survivors to suffer from cognitive function and occupational productivity for years post-treatment. Direct neuronal injury and disruption of central nervous system (CNS) folate homeostasis are the potential mechanisms of MTX-related neurotoxicity [7,8]. MTX neurotoxicity may present as encephalopathy, seizures, aphasia, and symptoms of strokes especially after high-dose oral administration or sustained low-dose therapy [9]. In addition, the drug is involved in mitochondrial dysfunction, which results in increased reactive oxygen species (ROS) that contribute to neurotoxic effects [10]. ROS-mediated peroxidation in cells eventually leads to the death of cells by apoptosis [10].

The hippocampus, part of the limbic system, plays a crucial role in learning and memory. The Dentate gyrus (DG) has three layers: granular, polymorphic, and molecular layers, and DG plays a role in receiving inputs for memory and mental processes [9]. Because the brain is highly metabolically active and has high polyunsaturated fatty acids, it is susceptible to damage by oxidative stress. Data collected so far suggest that memory impairments following chemotherapy often correlate with hippocampal dysfunction [11].

Various strategies aimed at reducing oxidative stress have suggested a neuroprotective effect against the deleterious effects of MTX. One of these strategies is using Moringa leaf extract (MLE), which is derived from the Moringa tree in the monogeneric family Moringaceae. These trees are broadly planted across tropical and subtropical regions of Asia and Africa. It has various applications (i.e., industrial, medicinal, and agricultural). Remarkably, moringa leaves contain approximately 25% to 32% raw protein [12]. All parts of the moringa plant are used in traditional medicine due to their anti-inflammatory and antioxidant properties. Moringa pterygosperma leaves are vitamin-rich, while the root extract has strong antimicrobial effects. Moringa oleifera leaves and seeds contain antioxidants, vitamins A, D, E, C, and γ-carotene [13]. MLE is used topically to relieve skin inflammation from bacterial and fungal infections or insect bites, and it has a low toxicity rate and a safety profile [12].

Thus, MLE has been proven to be benign even at higher consumption levels. Therefore, in this study, we investigate the neuroprotective effects of MLE against MTX-induced damage to the DS.

2. Materials and Methods

2.1. Ethics Approval

The experimental protocols, authorised by the Institutional Animal Care Committee of the Faculty of Medicine, Minia University, Egypt, no. 105/02/2024, implemented measures to minimise animal utilisation and discomfort. Procedures were executed expediently and with precision to mitigate stress-induced alterations.

2.2. Animals

This study utilized 48 adult male albino rats weighing between 130 and 170 grams and randomly divided them into four groups of twelve. All subjects were healthy and housed in hygienic, well-ventilated plastic cages with access to water and standard laboratory chow. A 12:12 light/dark cycle was maintained, with ambient laboratory temperatures between 24°C and 30°C. Following a seven-day acclimatization period, the experimental protocol commenced.

2.3. Drugs

Methotrexate procured from Minapharm Pharmaceuticals, Cairo, Egypt, was diluted in a freshly prepared physiological saline solution. The dosage regimen was set at 0.5 mg/kg, administered intraperitoneally (i.p.) twice weekly over four weeks [14]. MLE was collected from the El-Sheikh Zuwayed Station of the Desert Research Centre (North Sinai, Egypt) and prepared using an ethanolic extraction method as described in [15]. MLE was administered orally at a dose of 300 mg/kg body weight, twice weekly for four weeks [16].

2.4. Experimental Design

- Group 1 (Control): (n = 12) rats received a standard laboratory diet and water.
- Group 2 (MLE Positive Control): (n = 12) rats were treated with 300 mg/kg MLE through oral administration.
- Group 3 (MTX Treatment): (n = 12) rats received 0.5 mg/kg MTX via i.p. injection.
- Group 4 (MTX + MLE): (n = 12) rats received concurrent administration of 0.5 mg/kg MTX and 300 mg/kg MLE for the four weeks following the dosages and routes. After the fourth week, all rats were weighed and sub-

sequently euthanized via cervical dislocation. Their skulls were dissected, and their brains were meticulously extracted for further analysis.

2.5. Sampling

Brain tissues were extracted and sectioned into two halves for histological and immunohistochemical evaluations. One-half underwent preservation in 4% formaldehyde for 24 hours, followed by dehydration through graded alcohols and embedding in paraffin. For the second half, DG was extracted according to Hagihara et al. (2009) protocol [17], then was homogenized in a 20% (w/v) cold potassium phosphate buffer (0.01 M, pH 7.4) and centrifuged at 4 °C for 10 minutes at 2,795 *g* (Thermo Fisher Scientific, USA) superoxide dismutase (SOD) and malondialdehyde (MDA) levels were quantified from the supernatant.

2.6. Measurements of Oxidative Stress Parameters

SOD activity was determined using a colorimetric assay at a wavelength of 420 nm (Bio-Rad, USA). MDA concentration, indicative of lipid peroxidation, was assessed via thiobarbituric acid reactive substances, with results conveyed in equivalents of MDA, utilizing 1,1,3,3-tetramethoxypropane as a reference standard [18].

2.7. Histopathological Examination

Specimens were fixed in 10% formalin before paraffin embedding. Histological evaluations involved an independent pathologist analysing 3 µm sections stained with haematoxylin-eosin (H&E) and crystal violet using an Olympus microscope (Olympus, New Jersey, USA).

2.8. Histopathological Scoring of CNS Injury

The extent of microscopic lesions within the DG was quantified using a four-point grading system adapted from [19,20]:

- Grade 0: No detectable lesions
- Grade 1: Minimal lesions (< 15% of tissues)
- Grade 2: Mild lesions (15–45% of tissues)
- Grade 3: Moderate lesions (45–75% of tissues)
- Grade 4: Marked lesions (> 75% of tissues)

Histopathological changes noted included tissue oedema, red neuron presence, neuronal pyknosis, perineuronal oedema, neuronophagia of degenerated neurons, necrosis, and reactive gliosis.

2.9. Immunohistochemical Studies

Immunohistochemical analysis followed the methods detailed by Maae et al. [21]. Paraffin-embedded brain blocks were serially cut into 4 µm thick sections and mounted on positively charged glass slides for deparaffinization and rehydration. After trypsin treatment, slides were washed with PBS (phosphate-buffered saline). A 3% hydrogen peroxide solution and Ultra V Block mitigated nonspecific peroxidase binding. Sections were then incubated overnight with primary antibodies: Rabbit polyclonal Toll-like receptor 4 (TLR4) antibody (Catalog No. A11226, Abclonal Technology, dilution 1:100), essential for pathogen recognition and innate immunity activation; Rabbit polyclonal NLRP3 antibody (Catalog No. A12694, Abclonal Technology, dilution 1:100), involved in inflammation regulation, immune response, and apoptosis; and Rabbit polyclonal Caspase-1 antibody (Catalog No. A18646, Abclonal Technology).

2.10. Immunohistochemical Analysis of Brain Tissue Using Specific Antibodies

Following the protocols established by Maae et al. [21], paraffin-embedded brain tissue blocks were sectioned into 4 µm thickness and adhered to positively charged glass slides for subsequent deparaffinization and rehydration. The sections underwent trypsin incubation, followed by washing with phosphate-buffered saline (PBS). To mitigate nonspecific binding due to endogenous peroxidase, a 3% hydrogen peroxide solution was applied in conjunction with Ultra V Block. Primary antibodies were incubated overnight, comprising: Rabbit polyclonal TLR4 antibody

(Catalog No. A11226, Abclonal Technology, dilution 1:100), pivotal for pathogen identification and innate immune activation; Rabbit polyclonal NLRP3 antibody (Catalog No. A12694, Abclonal Technology, dilution 1:100), which is integral to inflammation regulation, immune response modulation, and apoptosis; Rabbit polyclonal Caspase-1 antibody (Catalog No. A18646, Abclonal Technology, dilution 1:100), crucial for apoptosis execution; and Rabbit polyclonal anti-glial fibrillary acidic protein (GFAP) antibody (Catalog No. FNab03426, Wuhan Fine Biotech Co., China, dilution 1:50), utilized to assess gliosis. Following incubation with the respective secondary antibodies (Lot and Company), the slides were counterstained with haematoxylin for 30 seconds, dehydrated, and mounted.

2.11. Neuronal Reactivity Scoring

Neurons in the DG exhibiting nuclear or cytoplasmic reactivity to antibodies were scored as positive. A semi-quantitative analysis was performed according to the modified Allred scoring system as described by [22]. Positive neuron counts were obtained within a 3 high power field (hpf) at 400x magnification utilizing ImageJ software [23], from which the mean ± standard error of the mean (SEM) was computed. Individual scores, reflecting the percentage of positive cells (0–5) and cytoplasmic staining intensity (0–3), were aggregated to provide final grades. Scoring thresholds for the percentage of positive cells were delineated as follows: score 1: < 10%, score 2: 10–20%, score 3: 20–50%, score 4: 50–70%, and score 5: > 70%. The intensity of cytoplasmic staining was scored as follows: score 1: weak, score 2: medium, score 3: strong.

2.12. Morphometric Studies

Assessment of intact granule cell counts and granular cell layer thickness was conducted at 400x magnification utilizing H&E-stained sections. The area percentage of immunopositivity for Caspase-1, GFAP, TLR4, and NLRP3 was quantified at equivalent magnification using image analysis software (ImageJ; https://rsbweb.nih.gov/ij/; NIH, Bethesda, MD). All morphometric metrics were evaluated across eight non-overlapping fields per rat among distinct experimental groups, with the histologist blinded to group assignments.

2.13. Statistical Analysis

Quantitative metrics, including rat body weight at experiment conclusion and MDA and SOD levels in immunoreactive cells, were subjected to analysis using GraphPad Prism software (version 9). Means and standard errors of the mean (SEM) were calculated for each group's parameters. Tukey-Kramer post hoc testing followed a one-way analysis of variance (ANOVA) to pinpoint significant intergroup differences, with results deemed statistically significant for $p < 0.05$.

3. Results and Discussion

3.1. Rat Body Weight

After the experiment, rats subjected to MTX significantly reduced body weight relative to both the control and MLE groups $p < 0.05$ [**Figure 1(a)**].

3.2. Assessment of Oxidative Stress Markers

Rats exposed to MTX demonstrated a statistically significant decrease in SOD levels ($p < 0.05$), coupled with markedly elevated MDA concentrations in brain tissue compared to control and MLE groups ($p < 0.05$). The MTX + MLE group significantly improved these oxidative stress markers [**Figures 1(b)** and **1(c)**].

3.3. Histopathological Results

Hematoxylin and eosin (H&E) staining of parasagittal sections of the DG revealed three distinct layers: molecular layer, granule cell layer, and polymorphic layer. The DG of the control group presented no signs of neuronal injury, characterized by well-organized granule cells arranged in dense columns with small, spherical nuclei and minimal interstitial space. The MLE group maintained a histological architecture similar to that of the control group. Conversely, the MTX-treated group showed significant histopathological alterations, including a reduced thickness of the granule cell layer compared to both control and MLE groups. The observation of red neurons, mononuclear inflammatory cells, and surrounding perineuronal oedema in the molecular layer was also noted. The MTX + MLE

group exhibited a granule cell layer that was nearly normal but still evidenced neuronal injury, indicated by perineuronal oedema and red neurons (**Figure 2** and **Table 1**).

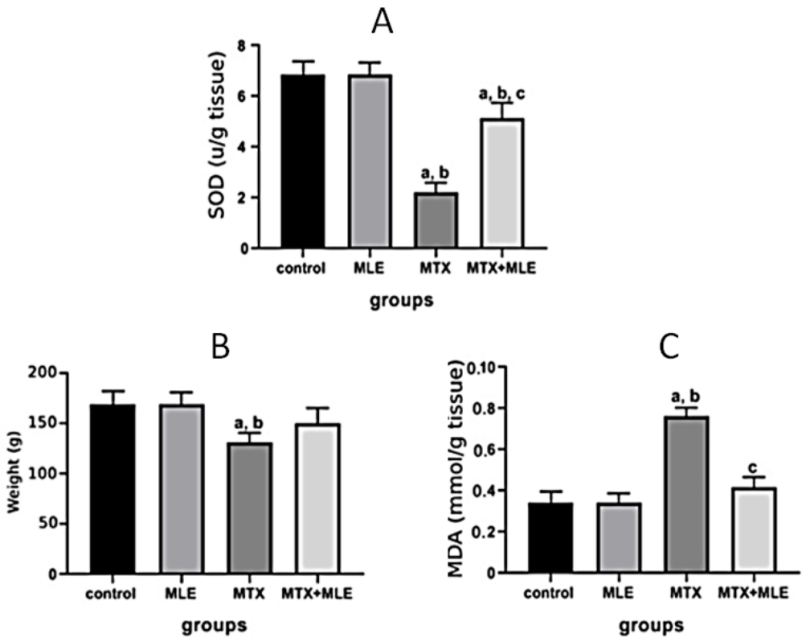

Figure 1. Quantitative analysis of rat body weight, MDA, and SOD, statistical comparisons between groups. Quantitative analysis of rat **(a)** body weight, **(b)** MDA and **(c)** SOD.

Note: Data are represented as mean ± SEM. **a:** Significant difference versus control group, **b:** Significant difference versus MLE group, **c:** Significant difference versus MTX group (Significant $p < 0.05$).

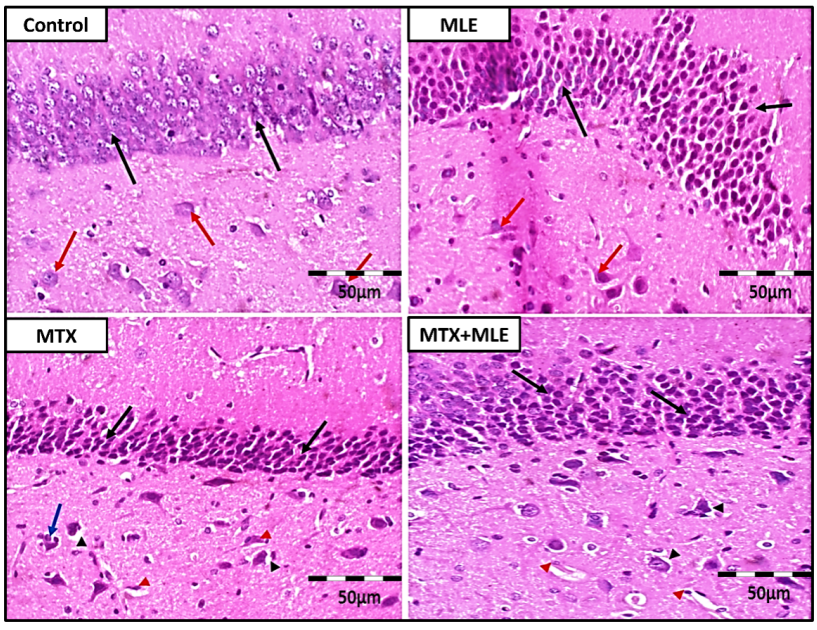

Figure 2. Representative photomicrographs of a parasagittal section of a control rat's DG, using H&E.

Note: C and MLE groups are showing uniform hippocampal area with no signs of neuronal injury, uniform granular cell layer neurons (Black arrows) and uniform molecular cell layer neurons (Red arrows). MTX group showing shrinkage in thickness of granular cell layer (Black arrows), perineuronal edema seen around molecular cell layer neurons (Black arrowheads), as well as red neurons (Red arrowhead) and mononuclear inflammatory cells infiltrate around neurons (Blue arrows). MLE + MTX group showing uniform hippocampal granular cell layer (Black arrows) with evidence of neuronal injury in neurons of molecular cell layer: perineuronal edema (Black arrowheads), as well as red neurons (Red arrowhead) (H&E, 400x).

Table 1. Histopathological scoring for brain tissue damage.

Groups	Brain
Control	0
MLE	0
MTX	Neuronal injury: Red neurons, peri-neuronal edema, inflammatory cells infiltrate. 60% of hippocampal area: Grade 3
MLE + MTX	Neuronal injury: Few red neurons and mild perineuronal edema. No inflammatory cells infiltrate. 10% of hippocampal area: Grade 1

Note: Extent of tissue damage using a four-point scale; as previously described: absent (grade 0) no lesions detected, minimal (grade 1) lesions involved less than 15% of the tissue section, mild (grade 2) lesions involved 15–45% of the tissue section, moderate (grade 3) lesions involved 45–75% of the tissue section, marked (grade 4) lesions involved greater than 75% of the tissue section.

3.4. Cresyl Violet Staining Results

Cresyl violet staining indicated that both control and MLE-treated groups displayed a uniform DG morphology, characterized by a dense granule cell layer and uniform neuronal architecture in the molecular layer. In contrast, granule cell neurons in the MTX group appeared shrunken, indicative of neurodegeneration and cell death. However, neurons in the MTX + MLE group largely retained their typical morphology, signalling a reduction in neurodegenerative histopathological findings (**Figure 3**).

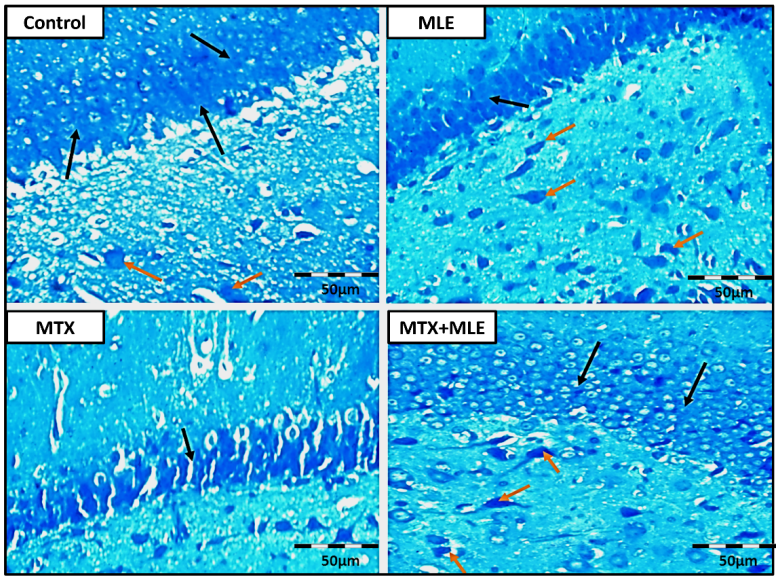

Figure 3. Representative photomicrographs of a parasagittal section of a control rat's DG, using Cresyl Violet.
Note: C and MLE groups are showing dense granular cell layer neurons (Black arrows) and uniform molecular cell layer neurons (Red arrows). MTX group is showing shrinkage in hippocampal granular cell layer neurons (Black arrows). MLE + MTX group showing dense granular cell layer neurons (Black arrows) and uniform molecular cell layer neurons (Red arrows) (Crystal violet, 400x).

3.5. Immunohistochemical Results

Immunohistochemical analysis indicated immunoreactivity through brown cytoplasmic and nuclear expression. TLR4 immunostaining revealed negative expression in both control and MLE-treated DG neurons. In contrast, focal TLR4 expression was present in the MTX group's granule cells and molecular layer neurons. Notably, TLR4 expression was absent in the MTX + MLE group (**Figure 4** and **Table 2**). Regarding NLRP3, both control and MLE groups exhibited negative immunoreactivity, contrasting with significant NLRP3 expression in the granule cell and molecular layer neurons in the MTX group ($p < 0.05$), which returned to negative in the MTX + MLE group (**Figure 4** and **Table 2**). For Caspase 1, the control and MLE groups were negative, while focal expression in granule cell layer neurons was observed in the MTX group, with negative expression in the MTX + MLE group (**Figure 5** and **Table 2**). GFAP immunostaining revealed positive cell scores of 3 with an intensity score of 2 in the control and MLE groups, whereas the MTX group exhibited 4 positive cells with the same intensity. The MTX + MLE group demonstrated a score of 3 for positive cells while maintaining an intensity score of 2 (**Figure 5** and **Table 2**).

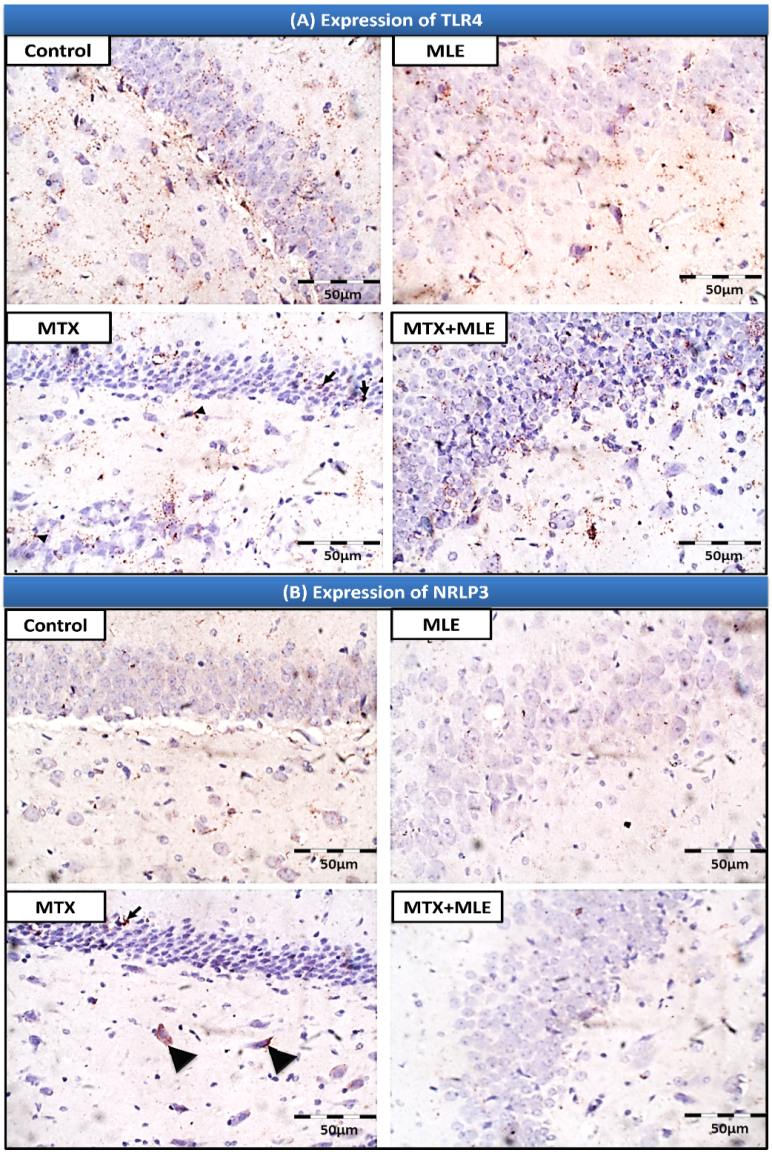

Figure 4. Representative photomicrographs of a parasagittal section of a control rat's DG. **(A)** C and MLE groups are showing negative expression of TLR4 in hippocampal neurons. **(B)** C and MLE groups are showing negative expression of NLRP3 in hippocampal neurons.

Note: (A) MTX group is showing focal expression of TLR4 in hippocampal granular cell layer neurons (Black arrows) and in molecular cell layer neurons (Black arrowheads). MLE+MTX group showing negative expression of TLR4 in hippocampal neurons. **(B)** MTX group is showing significant increase in the expression of NLRP3 in hippocampal granular cell layer neurons (Black arrows) and in molecular cell layer neurons (Black arrowheads). MLE+MTX group showing Negative expression of NLRP3 in hippocampal neurons (IHC, 400x).

Table 2. Scoring of immune-histochemical results.

Group	Anti-Caspase 1	Anti- GFAP	Anti- NLRP3	Anti- TLR4
Control	0	32 ± 5.3 (Score 3) Moderate (Score 2) Total score = 5	0	0
MLE	0	30.3 ± 3.5 (Score 3) Moderate (Score 2) Total score = 5	0	0
MTX	2.7 ± 2.5 (Score 1) Weak (Score 1) Total score = 2	50.7 ± 7.1 (Score 4) Moderate (Score 2) Total score = 6	2.7 ± 2.5 (Score 1) Weak (Score 1) Total score = 2	4 ± 2 (Score 1) Weak (Score 1) Total score = 2

Table 2. *Cont.*

Group	Anti-Caspase 1	Anti- GFAP	Anti- NLRP3	Anti- TLR4
MTX + MLE	0	24.7 ± 4.2 (Score 3) Moderate (Score 2) Total score = 5	0	0

Note: The percentage of positive cells was set as follows: 1-less than 10; 2-from 10 to 20; 3-from 20 to 50; 4-from 50 to 70; and score 5-more than 70. The staining intensity of positivity in the cytoplasm was scored as: 1-weak; 2-medium; and 3-strong.

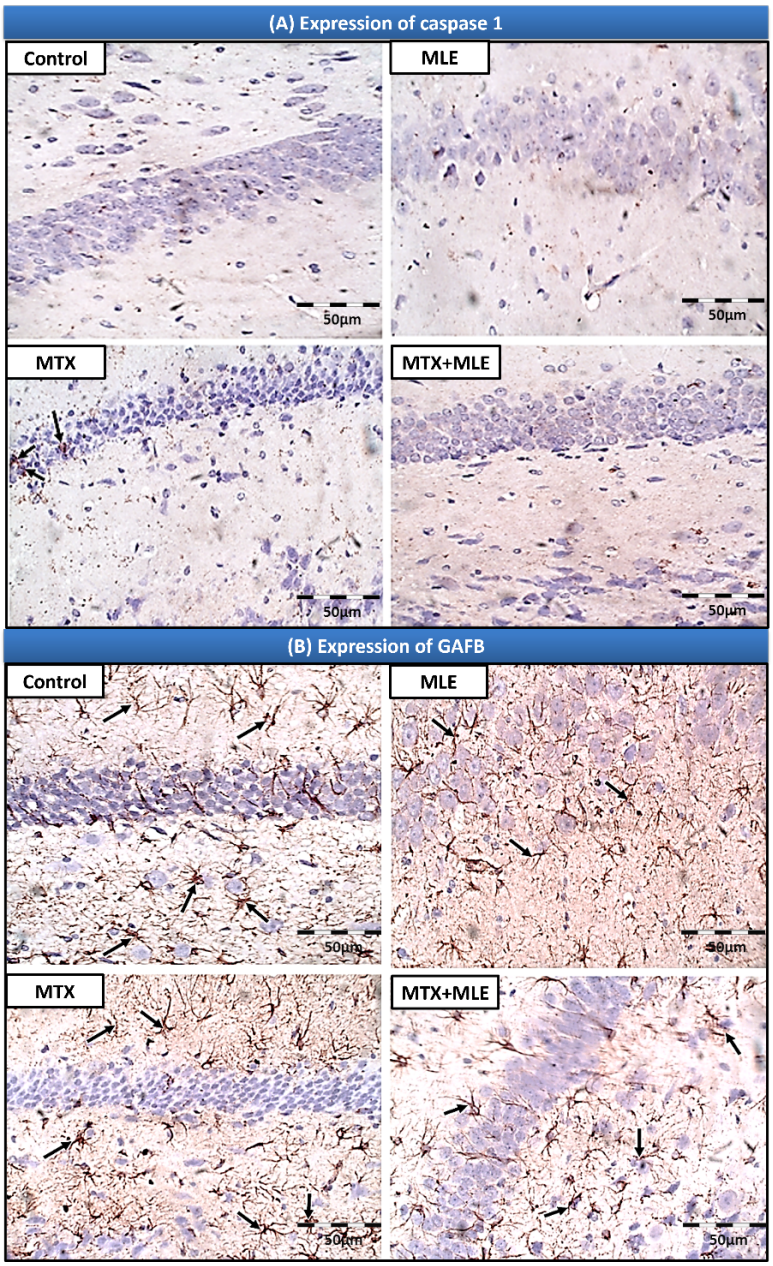

Figure 5. Representative photomicrographs of a parasagittal section of a control rat's DG. **(A)** C and MLE groups are showing negative expression of caspase 1 in hippocampal neurons. **(B)** C and MLE groups are showing positive expression of GFAP in astrocytes (Black arrows).

Note: (A) MTX group is showing focal expression of caspase 1 in hippocampal neurons (Black arrows). MLE + MTX group showing Negative expression of caspase 1 in hippocampal neurons, **(B)** MTX group is showing increased expression of GFAP in astrocytes (Black arrows). MLE + MTX group showing Positive expression of GFAP in astrocytes (IHC, 400x).

3.6. Morphometric Results

Morphometric analysis indicated that neither the number of granule cells nor the thickness of the granule cell layer differed significantly between control and MLE-treated groups. The MTX group's granule cell layer was significantly thinner than that of the control and MLE groups. The MLE + MTX group exhibited a substantial increase in granule cell number and layer thickness compared to the MTX group. However, these values remained lower than those of the control and MLE groups (**Figure 6** and **Table 3**). The morphometric evaluation of immunopositivity for TLR4, NLRP3, Caspase 1, and GFAP showed no significant differences between the control and MLE groups. However, the MTX group demonstrated significantly higher immunoreactivity than the control and MLE groups ($p < 0.05$). The MLE + MTX group exhibited significantly reduced immunoreactivity compared to the MTX group ($p < 0.05$) (**Figure 5** and **Table 3**).

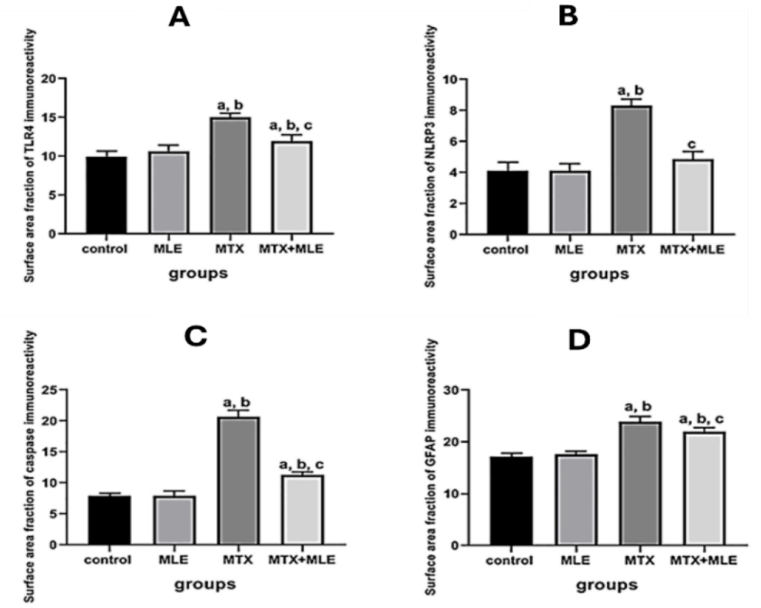

Figure 6. Quantitative analysis of TLR4, NLRP3, Caspase 1, and GFAP expression. Quantitative analysis of the mean area fraction (%) of positive cells of **(a)** TLR4, **(b)** NLRP3, **(c)** Caspase 1, and **(d)** GFAP.
Note: Data are represented as mean ± SEM. **a:** Significant difference versus control group, **b:** Significant difference versus MLE group, **c:** Significant difference versus MTX group (Significant $p < 0.05$).

Table 3. Scoring of morphometric results.

	Control	MLE	MTX	MTX + MLE
Granule cell layer thickness (µm)	63.8 ± 2.35	63.8 ± 2.1	26.2 ± 1.7 a,b	46.6 ± 2.7 a,b,c
Number of granule cells	116.4 ± 1.2	114.6 ± 1.4	85.6 ± 1.56 a,b	105.8 ± 1.66 a,b,c
Surface area fraction of caspase 1immunopositivity	7.9 ± 0.2	7.95 ± 0.34	20.6 ± 0.51 a,b	11.37 ± 0.19 a,b,c
Surface area fraction of NLRP3 immunopositivity	4.14 ± 0.23	4.14 ± 0.19	8.3 ± 0.2 a,b	4.86 ± 0.22 c
Surface area fraction of TLR4 immunopositivity	9.92 ± 0.34	10.69 ± 0.34	15.02 ± 0.24 a,b	11.99 ± 0.35 a,b,c
Surface area fraction of GFAP immunopositivity	17.14 ± 0.3	17.6 ± 0.28	23.9 ± 0.46 a,b	22.01 ± 0.35 a,b,c

Note: All parameters are expressed as mean ± SEM of 10 observations. Significant difference is considered when $p < 0.05$. **a:** Significant difference versus control group, **b:** Significant difference versus MLE group, **c:** Significant difference versus MTX group (Significant $p < 0.05$).

4. Discussion

Methotrexate is an anticancer agent that is also prescribed for diseases with an overactive immune system, like psoriasis and rheumatoid arthritis. The use of this medication is limited because it can cause harm to several parts of the body, mainly the nervous system. Accordingly, MLE contains properties that reduce inflammation and offer antioxidant benefits [24,25]. This study investigates the potential protective effects of MLE against MTX-induced neurotoxicity in male albino rats, suggesting that MLE may alleviate the adverse effects of MTX. Previous

research demonstrates that oestrogen can increase cell proliferation [26]; therefore, male albino rats were used in this study to minimize the effect of female hormones. Our findings indicated that MTX adversely affected rats, leading to weight loss along with alterations in the histological and immunohistochemical structure of neurons in the DG. This finding aligned with previous research findings as it showed that post-MTX treatment, rats experienced significant weight reduction [27]. The administration of MTX caused serious damage to the DG that included astrogliosis, inflammation, and apoptosis. However, giving MLE at a dosage of 300 mg/kg over four weeks greatly helped to resolve the structural damage induced by MTX. This is supported by previous research on MLE's neuroprotective effects against hypoxic damage [14] and MTX-induced neurodegeneration [28]. Moreover, MTX is shown to exacerbate oxidative imbalance in the brain by escalating ROS levels in parallel with decreasing the activity of important intracellular antioxidant enzymes. Specifically, the gene expression of the antioxidant response element (ARE) gene is being inhibited, thereby causing deactivation or depletion of antioxidant enzymes, leading to the accumulation of free radicals [29]. Consistent with this notion, MTX treatment led to elevation of brain MDA levels (a marker of lipid peroxidation and a measure of elevated ROS production) in parallel with a decrease of SOD levels. This dysregulation results in an environment with excessive free radical generation, but deficient antioxidant defence, which, in sum, leads to neuronal damage. Whereas treatment with MLE substantially ablated MTX provoked oxidative stress [30]. Co-administration of MLE and MTX in the present study caused MDA and SOD levels to revert to nearly baseline values. Moreover, studies have indicated that MLE prevents oxidation damage in many organs, such as the kidneys, liver, and gastrointestinal system [18,31]. This is supported by earlier research showing that after four weeks of MTX therapy, the level of SOD in the body decreases, probably because ROS initiates feedback behaviour or oxidative inactivation of SOD proteins [32]. There are many natural antioxidant enzymes, including SOD, which protect cells from damage caused by free radicals. A rise in tissue SOD is correlated with a more decisive antioxidant action. Histological analysis of the MLE-treated cohort improves our comprehension of MLE's potential neuroprotective effects on the hippocampal cellular structure. Notably, the preservation of granular cells in the DG supports the protective role of MLE. This finding aligns with previous studies that MLE helps limit hippocampal damage caused by MTX [28]. Similarly, other results noted frequent characteristic microstructures in the cerebral cortex of rats exposed to MLE [14]. Our investigation found that MLE helps to preserve the DG's structure intact, especially after the marked MTX-induced damage to the hippocampus. It appears that the apparent changes to the DG result from the effects of MTX treatment. Our results agree with previous research showing that MTX has a negative effect on brain structure, confirming our findings [33]. In this investigation, H&E and cresyl violet staining revealed specific degenerative changes in the DG following MTX treatment, including perineuronal oedema, loss of granular layer cells, accumulation of red neurons, and inflammatory cell infiltration around neurons. Wu et al. [33] reported that MTX treatment led to the presence of densely stained pyramidal neurons with areas of cell shrinkage. Earlier investigations revealed significant hydropic degeneration, distinct coagulative necrosis, and multiple pyknotic nuclei within the MTX group. These observations demonstrate that MTX causes histological alterations leading to cellular damage [18]. Based on our histological analysis in Group IV (MTX + MLE Simultaneously), MLE may mitigate specific alterations in DG neurons induced by MTX. Restoration of the cellular structure of the DG suggested that the use of MLE, parallel with MTX, may provide some neuroprotection against MTX-induced changes. According to existing evidence, co-administration of MLE with MTX may provide neuroprotection for the DG, emphasising MLE's potential therapeutic effects [18]. According to our findings, the thickness of the granular cell layer was significantly reduced, and the number of intact neurons in the DG was fewer in MTX-treated rats in comparison to the control and MLE groups. Applying Caspase-1 immunohistochemistry showed an increase in apoptosis and greater cell damage of neurons in the MTX cohort, also connected to a significant rise in neuronal damage. Observation of histopathological findings supports this by showing that MTX causes neurotoxic effects through increasing oxidative stress and damaging cells due to the lack of equilibrium in oxidant-antioxidant levels [32].

Antioxidant measures, for example, SOD are used to eliminate oxidizing radicals and change them into harmless species. If there is an imbalance in the production of ROS and antioxidant responses, oxidative stress happens, disrupting cellular function and possibly developing into many diseases [32]. Several studies point out that, besides oxidative stress, MTX-induced brain damage is also linked to the increased release of pro-inflammatory substances TNF-α, IL-1β, IL-6, and IL-18. Nevertheless, researchers are still figuring out how MTX causes toxicity [34]. In this investigation, TLR4 plays an important role in the progression of neurodegenerative diseases associated with MTX. TLR4 is a main PRR that starts the inflammatory process after detecting DAMPs from dying or stressed cells and

PAMPs present in Gram-negative bacteria. It is worth noting that TLR4 triggers ROS in the cells through NADPH oxidase, suggesting a link between ROS and TLR4. In addition, activation of TLR4 leads to NLRP3 inflammasome activation, which is responsive to oxidative stress. Cytosolic aggregates of NLRP3 contribute to neuroinflammation by activating caspase-1 and increasing the release of downstream cytokines, ultimately leading to neuronal death [35].

It was also noticed that, after MTX treatment, astrocytes became more active, as shown through the rise in GFAP expression. It is probably triggered by the damage to nearby neurons and the loss of cells caused by MTX, which is referred to as reactive gliosis. The analysis of GFAP in a tissue slide helped see how astrocytes responded to hurt neurons. Assessment of astrocyte cells in the sample gave an individual percentage score of 4, and the staining pattern had an intensity score of 2 for cytoplasmic positivity. MTX treatment resulted in a higher proportion of astrocytes showing GFAP in their cells when compared to the control group. The results found are consistent with other studies that note how astrocytes react to injury by producing more GFAP and being immunostained in experimental gliosis [36].

5. Conclusion

In conclusion, this study shows that Moringa leaf extract has a significant neuroprotective effect in Methotrexate neurotoxicity. Moringa leaf extract mitigates oxidative stress and inflammation via modulation of the TLR4 /NLRP3/caspase-1 signalling pathway to preserve the structural integrity of the dentate gyrus and provides a promising therapeutic strategy to improve the safety profile of Methotrexate treatment in malignancies. These results require further investigation to verify the possible clinical applications of Moringa leaf extract as a complementary therapy in cancer treatment regimens.

6. Limitations and Recommendations

While the findings highlight the neuroprotective potential of Moringa leaf extract, several limitations should be noted. First, the use of a single fixed dose (300 mg/kg) precludes insight into dose-response relationships and therapeutic margins. Future studies should incorporate multiple dosing regimens to determine efficacy thresholds and toxicity profiles. Second, the small sample size per group may limit statistical power and inflate effect sizes; larger cohorts are recommended to improve robustness. Lastly, the exclusive use of male rats limits generalizability, as sex-dependent differences in neuroinflammation and oxidative stress are well established. Including both sexes in future research will enhance translational relevance.

Author Contributions

Conceptualization, K.M.; methodology, K.M.; software, K.M.; validation, K.M.; formal analysis, K.M.; investigation, K.M.; resources, K.M.; data curation, K.M.; writing—original draft preparation, K.M.; writing—review and editing, K.M.; visualization, K.M.; supervision, K.M.; project administration, K.M.; funding acquisition, Y.Y. All authors have read and agreed to the published version of the manuscript.

Funding

This work received no external funding.

Institutional Review Board Statement

The animal study protocol was approved by the Ethics Committee of the Faculty of Medicine, Minia University, Egypt no.:1501-02/2024, date 13/02/ 2024, the study implemented measures to minimise animal utilisation and discomfort. Procedures were executed expediently and with precision to mitigate stress-induced alterations.

Informed Consent Statement

Not applicable.

Data Availability Statement

The datasets generated and analyzed during the present study are available from the corresponding author upon reasonable request.

Conflicts of Interest

The authors declare no conflict of interest.

References

1. Ahmed, Z.S.O.; Hussein, S.; Ghandour, R.A.; et al. Evaluation of the Effect of Methotrexate on the Hippocampus, Cerebellum, Liver, and Kidneys of Adult Male Albino Rat: Histopathological, Immunohistochemical and Biochemical Studies. *Acta Histochem.* **2021**, *123*, 151682.
2. Koźmiński, P.; Halik, P.K.; Chesori, R.; et al. Overview of Dual-Acting Drug Methotrexate in Different Neurological Diseases, Autoimmune Pathologies and Cancers. *Int. J. Mol. Sci.* **2020**, *21*, 3483.
3. Liu, H.; Wan, H.; Zhang, A.; et al. Polypyrrole-Ferric Phosphate-Methotrexate Nanoparticles Enhance Apoptosis/Ferroptosis of M1 Macrophages via Autophagy Blockage for Rheumatoid Arthritis Treatment. *J. Nanobiotechnol.* **2025**, *23*, 428.
4. Salwa, M.O.; Dorria, A.M.; Ahlam, W.M.; et al. The Toxic Effects of Methotrexate on the Cerebellar Cortex of Adult Albino Rats and the Protective Role of Vitamin C: A Light Microscopic Study. *Med. J. Cairo Univ.* **2021**, *89*, 2131–2136.
5. Karpa, V.; Kalinderi, K.; Fidani, L.; et al. Association of MicroRNA Polymorphisms With Toxicities Induced by Methotrexate in Children With Acute Lymphoblastic Leukemia. *Hematol. Rep.* **2023**, *15*, 634–650.
6. Yuksel, Y.; Yuksel, R.; Yagmurca, M.; et al. Effects of Quercetin on Methotrexate-Induced Nephrotoxicity in Rats. *Hum. Exp. Toxicol.* **2017**, *36*, 51–61.
7. Hwang, S.Y.; Kim, K.; Ha, B.; et al. Neurocognitive Effects of Chemotherapy for Colorectal Cancer: A Systematic Review and a Meta-Analysis of 11 Studies. *Cancer Res. Treat.* **2021**, *53*, 1134–1147.
8. Li, W.; Mo, J.; Yang, Z.; et al. Risk Factors Associated With High-Dose Methotrexate Induced Toxicities. *Expert Opin. Drug Metab. Toxicol.* **2024**, *20*, 263–274.
9. Ayuob, N.N.; El Wahab, M.G.A.; Ali, S.S.; et al. Ocimum basilicum Improve Chronic Stress-Induced Neurodegenerative Changes in Mice Hippocampus. *Metab. Brain Dis.* **2018**, *33*, 795–804.
10. Kolli, V.K.; Natarajan, K.; Isaac, B.; et al. Mitochondrial Dysfunction and Respiratory Chain Defects in a Rodent Model of Methotrexate-Induced Enteritis. *Hum. Exp. Toxicol.* **2014**, *33*, 1051–1065.
11. Nogueira, E.; Sárria, M.P.; Azoia, N.G.; et al. Internalization of Methotrexate Conjugates by Folate Receptor-α. *Biochemistry* **2018**, *57*, 6780–6786.
12. Qamar, H.; Rehman, S.; Chauhan, D.K. Current Status and Future Perspective for Research on Medicinal Plants With Anticancerous Activity and Minimum Cytotoxic Value. *Curr. Drug Targets* **2019**, *20*, 1227–1243.
13. Cuellar-Nuñez, M.L.; Luzardo-Ocampo, I.; Campos-Vega, R.; et al. Physicochemical and Nutraceutical Properties of Moringa (Moringa oleifera) Leaves and Their Effects in an In Vivo AOM/DSS-Induced Colorectal Carcinogenesis Model. *Food Res. Int.* **2018**, *105*, 159–168.
14. Mohamed, A.A.R.; Metwally, M.M.M.; Khalil, S.R.; et al. Moringa oleifera Extract Attenuates the $CoCl_2$ Induced Hypoxia of Rat's Brain: Expression Pattern of HIF-1α, NF-kB, MAO and EPO. *Biomed. Pharmacother.* **2019**, *109*, 1688–1697.
15. Batmomolin, A.; Ahsan, A.; Wiyasa, I.W.A.; et al. Ethanolic Extract of Moringa oleifera Leaves Improve Inflammation, Angiogenesis, and Blood Pressure in Rat Model of Preeclampsia. *J. Appl. Pharm. Sci.* **2020**, *10*, 52–57.
16. Farid, A.S.; Hegazy, A.M. Ameliorative Effects of Moringa oleifera Leaf Extract on Levofloxacin-Induced Hepatic Toxicity in Rats. *Drug Chem. Toxicol.* **2020**, *43*, 616–622.
17. Hagihara, H.; Toyama, K.; Yamasaki, N.; et al. Dissection of Hippocampal Dentate Gyrus From Adult Mouse. *J. Vis. Exp.* **2009**, *33*, 1543.
18. Soliman, M.M.; Aldhahrani, A.; Alkhedaide, A.; et al. The Ameliorative Impacts of Moringa Oleifera Leaf Extract Against Oxidative Stress and Methotrexate-Induced Hepato-Renal Dysfunction. *Biomed. Pharmacother.* **2020**, *128*, 110259.
19. Klopfleisch, R. Multiparametric and Semiquantitative Scoring Systems for the Evaluation of Mouse Model Histopathology—A Systematic Review. *BMC Vet. Res.* **2013**, *9*, 1–15.

20. Yip, P.K.; Hasan, S.; Liu, Z.H.; et al. Characterisation of Severe Traumatic Brain Injury Severity From Fresh Cerebral Biopsy of Living Patients: An Immunohistochemical Study. *Biomedicines* **2022**, *10*, 518.
21. Maae, E.; Nielsen, M.; Steffensen, K.D.; et al. Estimation of Immunohistochemical Expression of VEGF in Ductal Carcinomas of the Breast. *J. Histochem. Cytochem.* **2011**, *59*, 750–760.
22. Ilić, I.R.; Stojanović, N.M.; Radulović, N.S.; et al. The Quantitative ER Immunohistochemical Analysis in Breast Cancer: Detecting the 3+0, 4+0, and 5+0 Allred Score Cases. *Medicina* **2019**, *55*, 461.
23. Schneider, T.; Przewłocki, R. Behavioral Alterations in Rats Prenatally Exposed to Valproic Acid: Animal Model of Autism. *Neuropsychopharmacology* **2005**, *30*, 80–89.
24. Hasan, R.R.A.; Al-Gareeb, A.I. The Protective Effect of Alfa Lipoic Acid Against Methotrexate-Induced Acute Liver Injury in Mice. *Biochem. Cell Arch.* **2022**, *22*, 3885–3892.
25. Armagan, I.; Bayram, D.; Candan, I.A.; et al. Effects of Pentoxifylline and Alpha Lipoic Acid on Methotrexate-Induced Damage in Liver and Kidney of Rats. *Environ. Toxicol. Pharmacol.* **2015**, *39*, 1122–1131.
26. Tanapat, P.; Hastings, N.B.; Reeves, A.J.; et al. Estrogen Stimulates a Transient Increase in the Number of New Neurons in the Dentate Gyrus of the Adult Female Rat. *J. Neurosci.* **1999**, *19*, 5792–5801.
27. Elsawy, H.; Alzahrani, A.M.; Alfwuaires, M.; et al. Nephroprotective Effect of Naringin in Methotrexate-Induced Renal Toxicity in Male Rats. *Biomed. Pharmacother.* **2021**, *143*, 112180.
28. Hussein, Y. Histological and Immunohistochemical Changes in the Hippocampus of the Adult Male Albino Rats Treated With Amethopterin and the Possible Protective Role of Moringa Leaves Extract. *Egypt. J. Anat.* **2017**, *40*, 294–300.
29. Ebrahimi, R.; Sepand, M.R.; Seyednejad, S.A.; et al. Ellagic Acid Reduces Methotrexate-Induced Apoptosis and Mitochondrial Dysfunction via Up-Regulating Nrf2 Expression and Inhibiting the IκBα/NFκB in Rats. *DARU J. Pharm. Sci.* **2019**, *27*, 721–733.
30. Noubissi, P.A.; Njilifac, Q.; Tagne, M.A.F.; et al. Protective Effects of Moringa Oleifera Against Acetic Acid-Induced Colitis in Rat: Inflammatory Mediators' Inhibition and Preservation of the Colon Morphohistology. *Pharmacol. Res. Nat. Prod.* **2024**, *3*, 100038.
31. Minaiyan, M.; Asghari, G.; Taheri, D.; et al. Anti-Inflammatory Effect of Moringa Oleifera Lam. Seeds on Acetic Acid-Induced Acute Colitis in Rats. *Avicenna J. Phytomed.* **2014**, *4*, 127–136.
32. Abdel-Daim, M.M.; Khalifa, H.A.; Abushouk, A.I.; et al. Diosmin Attenuates Methotrexate-Induced Hepatic, Renal, and Cardiac Injury: A Biochemical and Histopathological Study in Mice. *Oxid. Med. Cell. Longev.* **2017**, *2017*, 3281670.
33. Wu, L.L.; Lin, D.N.; Yu, L.H.; et al. Endoplasmic Reticulum Stress Plays an Important Role in Methotrexate-Related Cognitive Impairment in Adult Rats. *Int. J. Clin. Exp. Pathol.* **2017**, *10*, 10252–10260.
34. Molteni, M.; Gemma, S.; Rossetti, C. The Role of Toll-Like Receptor 4 in Infectious and Noninfectious Inflammation. *Mediators Inflamm.* **2016**, *2016*, 6978936.
35. Zhang, L.; Tang, Y.; Huang, P.; et al. Role of NLRP3 Inflammasome in Central Nervous System Diseases. *Cell Biosci.* **2024**, *14*, 75.
36. Arici, S.; Karaman, S.; Dogru, S.; et al. Central Nervous System Toxicity After Acute Oral Formaldehyde Exposure in Rabbits: An Experimental Study. *Hum. Exp. Toxicol.* **2014**, *33*, 1141–1149.